Sources of Continuous GW Radiation: Implications to Physics and Astrophysics

LIGO Science Workshop, ICTS-TIFR, Bengaluru
27–28 October, 2023

Arunava Mukherjee
DAE-Saha Institute of Nuclear Physics (SINP), HBNI

LIGO-G2302108-v3

CW Signals: a Few Scientific Motivations

How is it different from CBC signals?

- Compact binary coalescence (CBC) signals have been proved an excellent tool:
    - To test of general relativity (TGR)

      B. P. Abbott, et al. PRL, 116, Issue 22, id.221101 (2016);
      B. P. Abbott, et al. PRL, 123, Issue 1, id.011102 (2019);
      B. P. Abbott, et al. PRD, 103, Issue 12, id.122002 (2021)
    - To constrain dense matter physics under extreme conditions, e.g., NS EOS

      B. P. Abbott, et al. PRL, 119, Issue 16, id.161101 (2017);
      B. P. Abbott, et al. PRL, 121, Issue 16, id.161101 (2018);
      B. P. Abbott, et al. PRX, 9, Issue 1, id.011001 (2019)
- CW signal is **persistent**, as opposed to transient CBC signals
- Useful for **precision tests** of certain aspects of TGR and Extreme Matter Physics
- **Reliability** and **reproducibility** of results
- **Assured improvements** in science results in future with **ever increasing SNR**

Continuous Gravitational Wave Radiations

Sources and Mechanisms

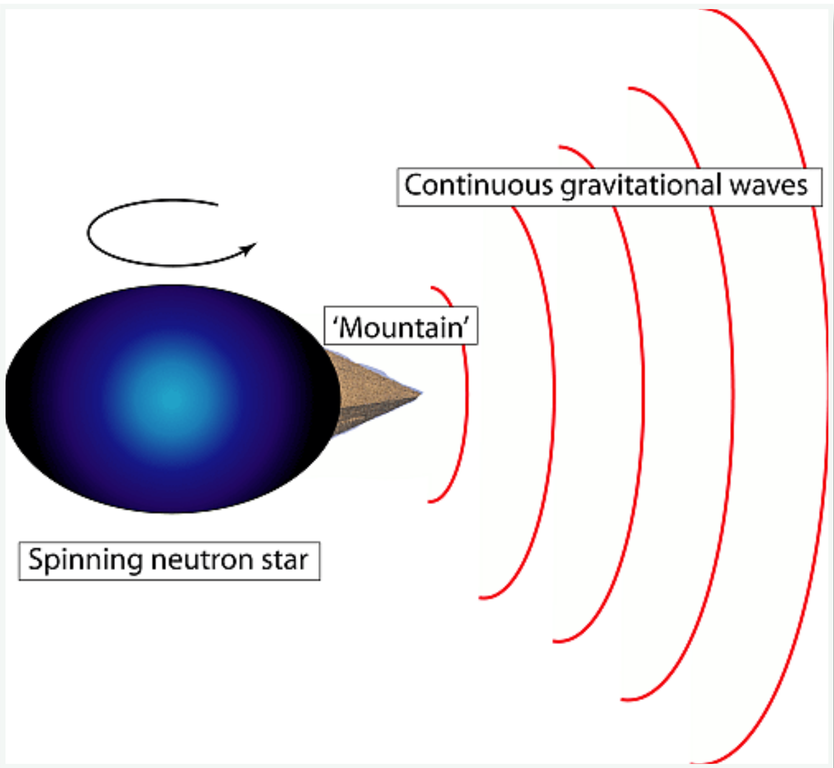

Non-axisymmetric spinning neutron stars

Freely precessing triaxial NS

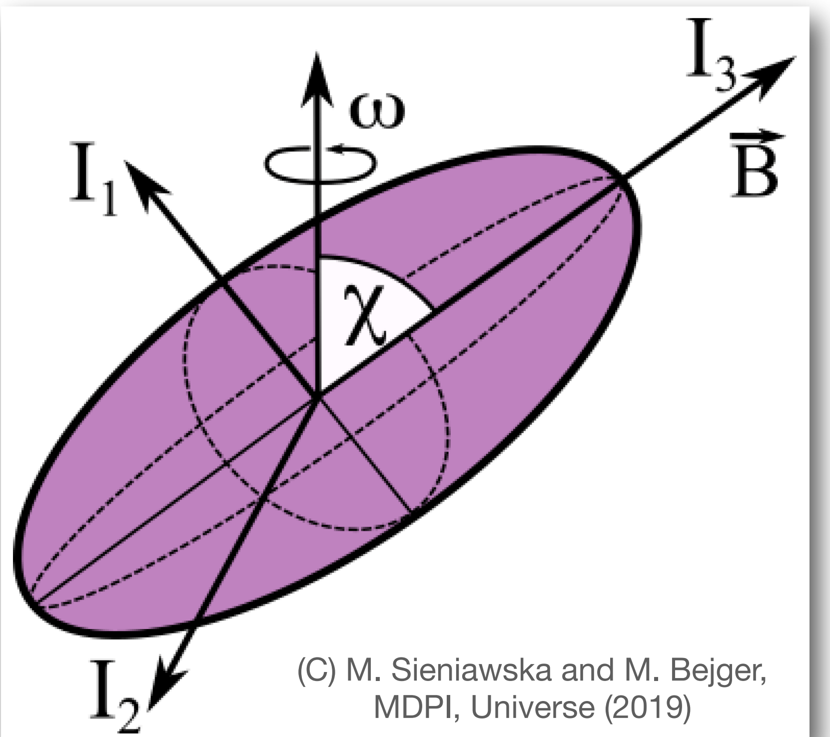

CFS instabilities, e.g., r-mode

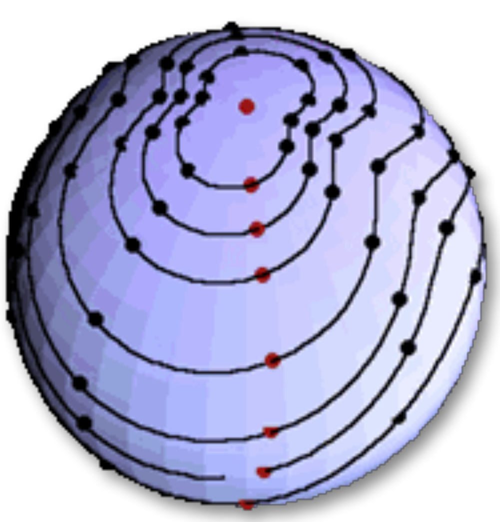

(Courtesy of C. Hanna and B. Owen, Penn State)

Dark matter/Boson clouds around BH

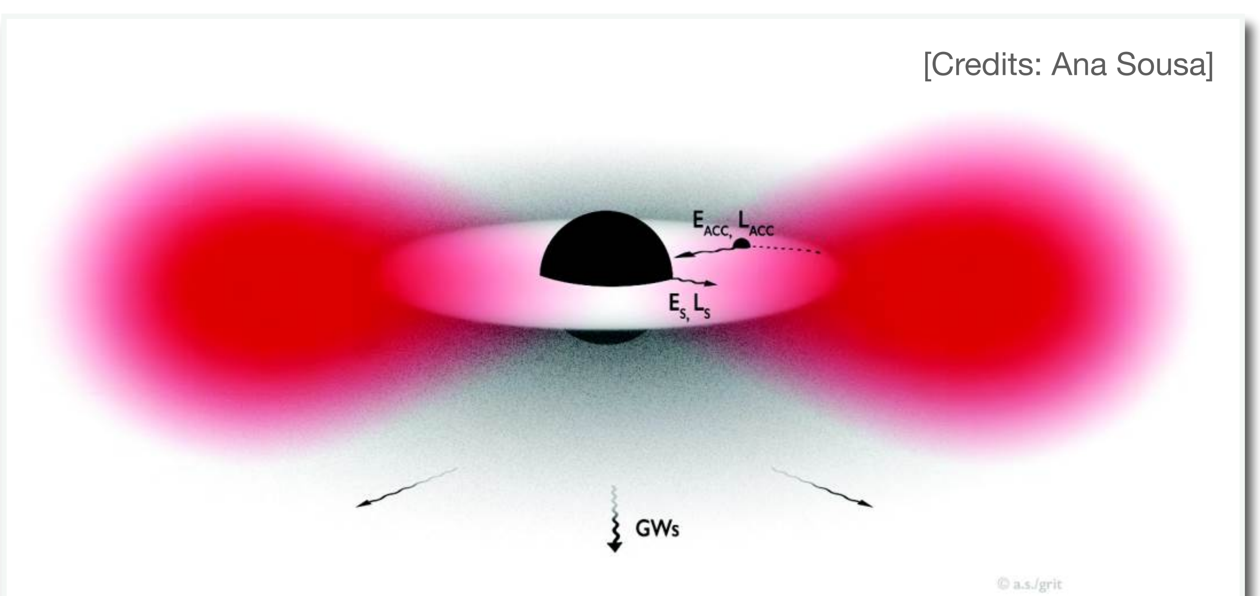

Source: https://cqgplus.com/2015/06/11/black-hole-superradiance-and-the-hunt-for-dark-matter/

Rapidly spinning deformed neutron stars

CW Sources & Emission Mechanism I

- Consider a non-axisymmetric neutron star with mis-aligned rotation axis (say, z-axis)

- The ellipticity (ε) of the star is defined as:

$$\epsilon = \frac{I_{xx} - I_{yy}}{I_{zz}}$$

- For l = m = 2 mode, continuous gravitational wave (CW) frequency $f_{GW} = 2 \times f_{spin}$

- GW-strain amplitude (h) is given by:

$$h_0 = \frac{4\pi^2 G}{c^4}\frac{I_{zz} f_{gw}^2}{d}\epsilon = 10^{-26}\left(\frac{\epsilon}{10^{-6}}\right)\left(\frac{f_{gw}}{100\ \mathrm{Hz}}\right)^2\left(\frac{d}{1\ \mathrm{kpc}}\right)^{-1}$$

- Gravitational wave power and spin-down is given by:

$$\frac{dE_{\rm rot}}{dt} = -\frac{32G}{5C^5}\,\epsilon^2 I_3^2 \omega_{\rm rot}^6.$$

$$\dot{\omega}_{\rm rot} = -\frac{32G}{5c^5}\,\epsilon^2 I_3 \omega_{\rm rot}^5.$$

NS Quasi Normal Modes, CFS Instability

CW Sources & Emission Mechanism II

- CFS (Chandrasekhar-Friedman-Schutz) instabilities are strong candidates to emit detectable CW signals in the near future

S. Chandrasekhar (1970);
Friedman and Schutz (1975, 1978)

- Depending on the intrinsic and extrinsic properties, a NS can have various QNMs (non-radial modes) that becomes CFS unstable due to GW emission

    - f-mode (fundamental mode) ⟶ fluid oscillation modes due to pressure gradient, e.g., *supernovae*, *BNS mergers*, etc. ⟶ freq range ~ 2.2 – 4 kHz

      Andersson & Kokkotas (1998)

    - r-mode (Rossby wave) ⟶ restoring force: coriolis force ⟶ freq range ~ (4/3 * f_{spin} + GR correction from NS EOS)

      L. Lee, et al. (1998); B. Owen, et al. (1998);
      N. Andersson (1998)

    - g-mode (gravity waves) ⟶ restoring force: buoyancy/gravity driven ⟶ freq range ~ 100 – 200 Hz

Dark Matter/Bosonic Clouds Around BHs

CW Sources & Emission Mechanism III

- **Ultralight Bosons** (axion-like dark matter candidates) can be found in large amount around **spinning black holes**

Arvanitaki et al. 2010; Baumann et al. 2019

- These particles could be spontaneously created via **energy extraction** from BH's spin using **Penrose process**. There could be two intriguing channels:

1. Axions can **annihilate with each other** to produce gravitons with frequency $f_{graviton} = 2m_{axion}c^2/h$

Arvanitaki et al. 2015; K. Riles, 2023

2. Emission occurs through the **level transition of quanta** in the Boson cloud. This becomes plausible when:

   A. those particles form **Bose condensation** around the BHs

   B. Compton wavelength of axion

$$\lambda = \frac{h}{m_{axion}c} \gtrapprox \frac{4\pi G M_{BH}}{c^2} \implies m_{axion} \lessapprox = (7 \times 10^{-11} eV/c^2)\frac{M_\odot}{M_{BH}}$$

Arvanitaki et al. 2015; Baumann et al. 2019; K. Riles, 2023

Implications to Fundamental Physics & Astrophysics

Implications to Test of General Relativity

Polarisation Tests of Alternate Theories of Gravity

- **In GR**: gravitational wave propagating in Z-direction looks in transverse traceless gauge (TT-gauge):

$$(A^{TT}_{\alpha\beta}) = \begin{pmatrix} 0 & 0 & 0 & 0 \\ 0 & A_{xx} & A_{xy} & 0 \\ 0 & A_{xy} & -Axx & 0 \\ 0 & 0 & 0 & 0 \end{pmatrix}$$

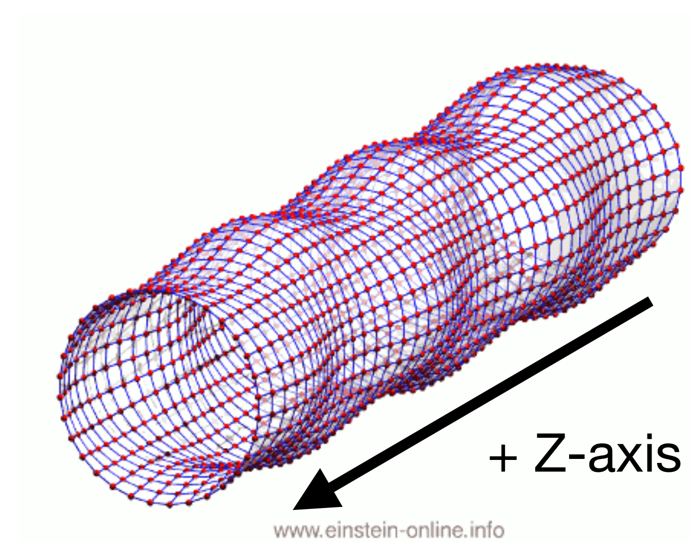

- It predicts **two independent polarisation** modes for GW: '+' & 'x' polarisation

- Long duration continuous gravitational wave (CW) signals are **excellent tools** to determine/ constrain **GW-polarisation** modes

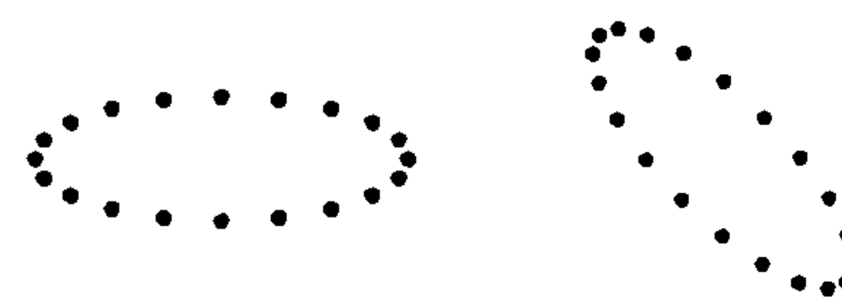

Non-Tensorial Polarisations Beyond GR

Testing Modified/non-GR Theory of Gravity

- Alternate theories of gravity predicts other (non-tensorial) polarisation modes
- In general, there could be **six independent polarisation modes** of a gravitational waves in other theories of gravity (i.e, modified General Relativity OR **Mod-GR**)

For GW propagating in Z-directions:

$$\begin{pmatrix} A_b + A_+ & A_\times & A_{Vx} \\ A_\times & A_b - A_+ & A_{Vy} \\ A_{Vx} & A_{Vy} & A_l \end{pmatrix}$$

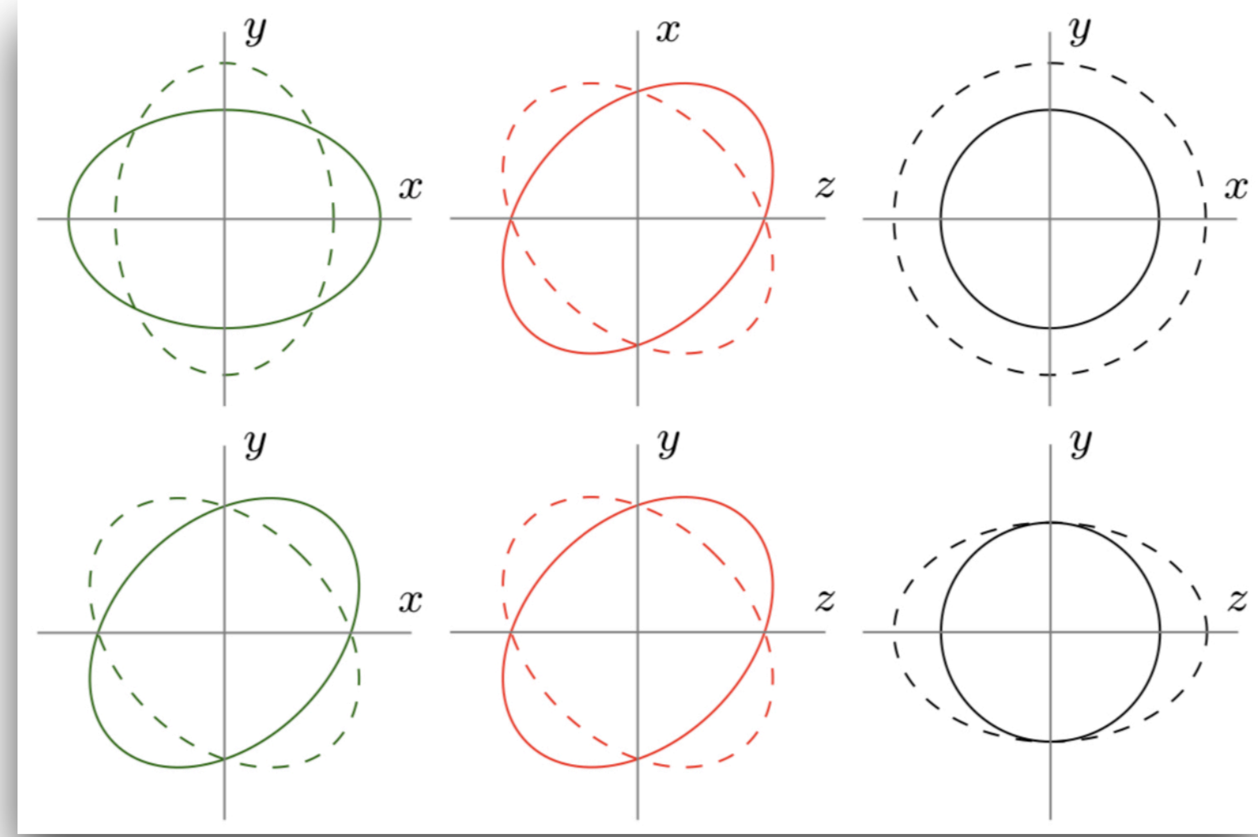

Effect of 6 different polarisation modes on matter

Theories	Polarization modes
Metric $f(R)$ gravity	$+, \times, b, l$
Palatini $f(R)$ gravity	$+, \times$
Scalar-tensor theory (massive)	$+, \times, b, l$
Brans-Dicke theory (massive)	$+, \times, b, l$
Brans-Dicke theory (massless)	$+, \times, b$

CW signals are promising tool to find the polarisation modes

Implications to Physics and Astrophysics

Properties of NS & Extreme Matter Physics

- GW170817 (CBC/BNS source) provided a constraint on NE EOS
- A CW-signal can be used for **much stricter constraints** (e.g., r-mode, g-mode) on the EOS parameter space and the composition of dense β-equilibrium matter
- A proper identification of **NS ellipticity** can shed light on the properties of **crustal physics**:
    - direct/modified **URCA** processes (*connecting to Astroparticle Physics!*) ⟶ deep crustal heating ⟶ "thermal mountain" (?!)
    - Geometry and distribution of **magnetic fields inside** the star
    - **Inhomogeneity** caused to the neutron star by **accretion process**
    - Indirect detection of **dark matter** (if lucky!), or constraints on parameter space
- Precision test on the **propagation effects of gravitons** w.r.t. photons (in combination of EM-observations)

Challenges
&
Opportunities

Challenges in CW Detection

Computational cost for wide parameter space searches

- CW signals are extremely weak ⟶ needs very long observation time ⟶ can quickly become computationally expensive (*see David's talk next*)

- Often we have only **partial/no knowledge of the source properties** (e.g., spin freq, and its time-derivatives, sky position, etc.) ⟶ computational cost increases

Leaci & Prix (2015)

- Spinning NS in a **binary system** — which could be more interesting — can further increase the computational cost

- NS in **accreting LMXB** systems can be promising: but fluctuating accretion rate cause loss in coherence due to **spin-wandering** effect

AM, Messenger, Riles (2018)

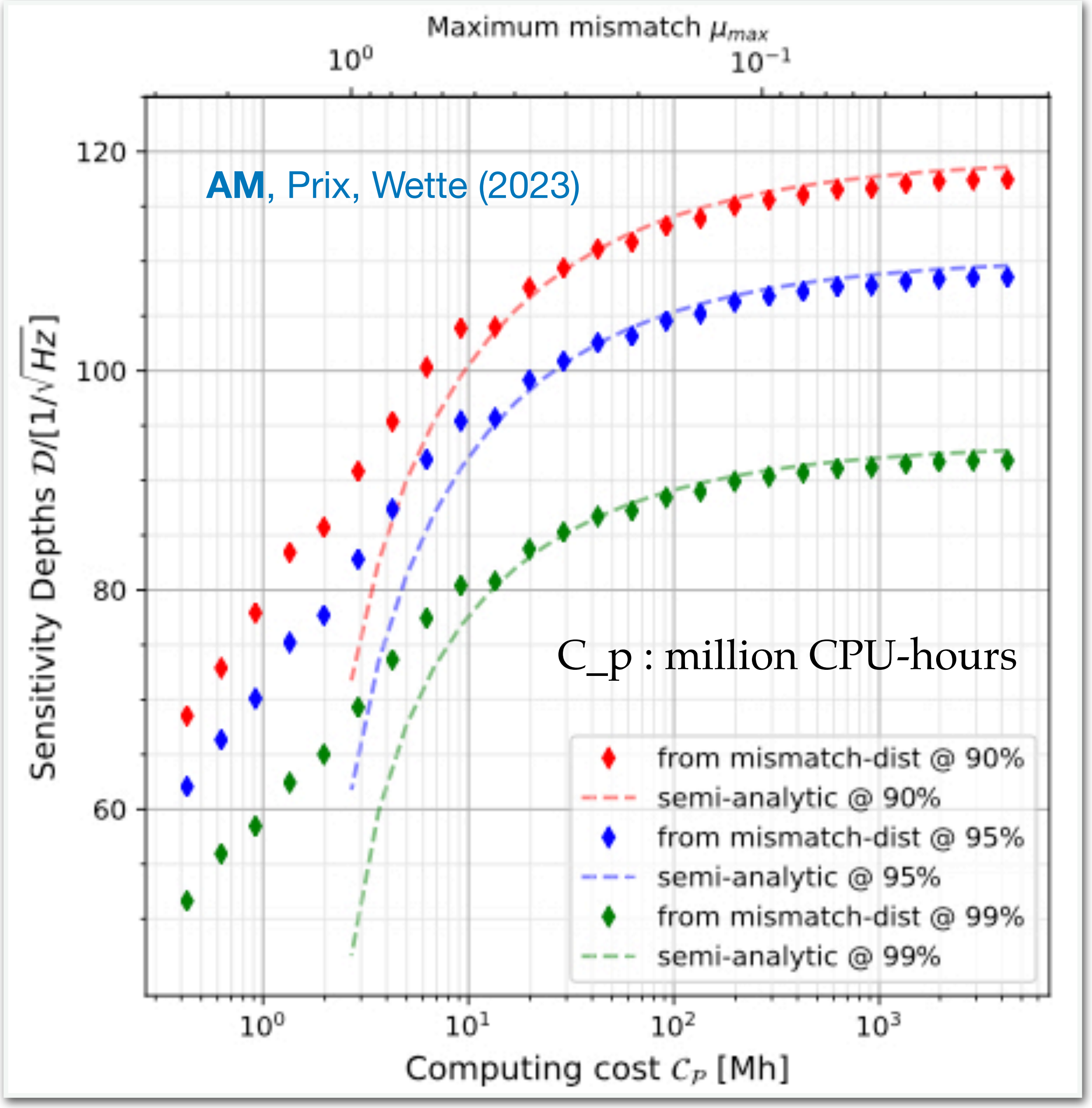

Usefulness of Additional GW-Detectors

Importance of LIGO-India

- **Semi-coherent** searches are the most intriguing ones ⟶ they have the potential for the **strong statistical detection** of a CW signal

- **Computational cost** increases as a **steep power** of observational duration for any search

Curtesy: LSC & LIGO-CalTech

- On the contrary, adding more detectors only **marginally increases** the computational cost —> **adding LIGO-India will be useful**!

Benefits of EM (X-Ray, Radio) Observations

Increase in Detection Sensitivity

- Electromagnetic observations can significantly reduce the search parameter space
  - It results in much lower computing cost
  - It reduces the false-alarm probability
  - It can significantly increases the search sensitivity => detection probability
  - Systematic monitoring of glitching pulsars will be important and useful for CW searches
  - **Simultaneous X-ray/radio/optical observations of interesting CW sources could be highly rewarding!**

Scope of Indian Observational Facilities

Synergising EM Astronomy Community

GMRT (Courtesy: NCRA-TIFR)

India has several excellent radio & X-ray telescopes (at present and possibly in future)

ASTROSAT (Courtesy: ISRO/TIFR)

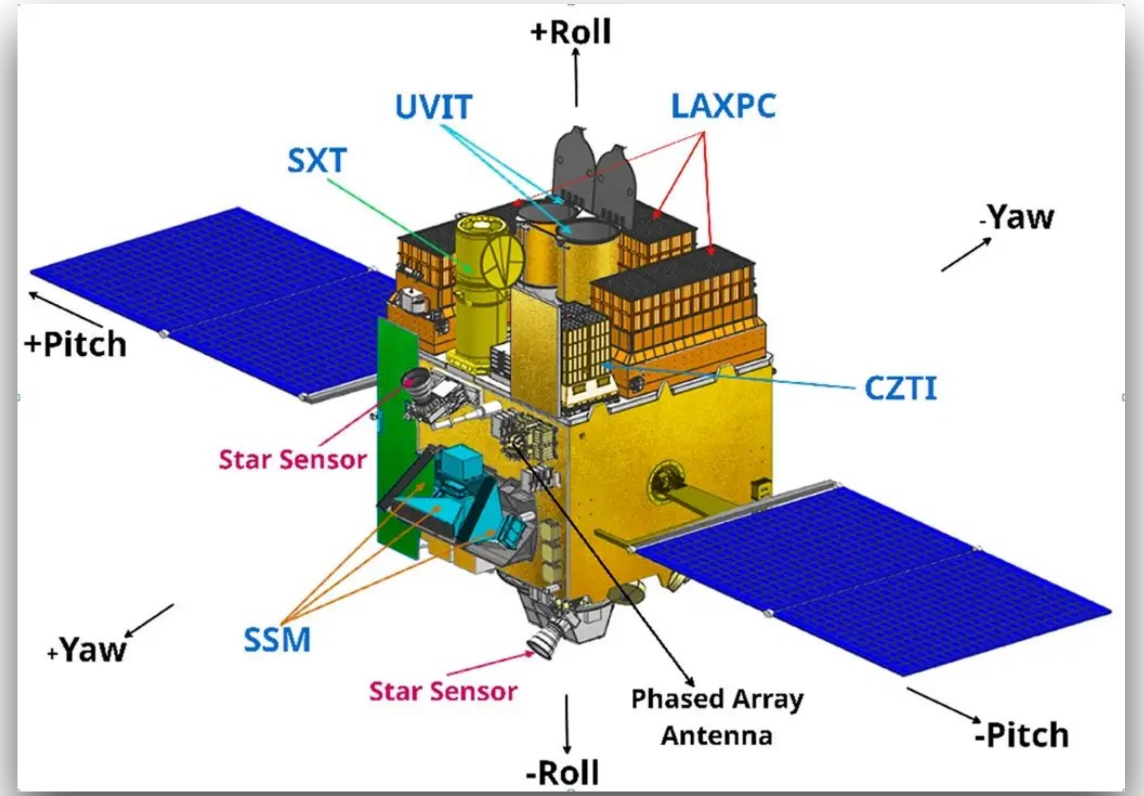

A coordinated and planned observations of interesting/promising targets could be extremely beneficial!

ORT (Courtesy: NCRA-TIFR)

Thank You!

We Encourage Comments & Discussions
After Both the Presentations

Backup Slides

Different Observational Scenarios

EM Observations Can Constrain Some of the Source Parameters

TABLE I. Different parameter-space search regions considered for Sco X-1. Note that $\mathcal{P}_0$ has been used in this study as a test range for various Monte Carlo tests of BINARYWEAVE, and $\mathcal{P}_{1-3}$ represent observational constraints considered in recent CW searches and studies. In addition, various combinations of parameter ranges are considered, $\mathcal{P}_{4-21}$, in order to explore the impact of improved observation constraints and reduced search ranges.

Search space $\mathcal{P}$	f [Hz]	a_p [ls]	P_{orb} [s]	t_{asc} [GPS s]	Reference(s)/Comment(s)
$\mathcal{P}_0$	10–700	0.3–3.5	68023.7 ± 0.2	1124044455.0 ± 1000	BINARYWEAVE test range
$\mathcal{P}_1$	20–500	1.26–1.62	68023.70496 ± 0.0432	897753994 ± 100	Leaci and Prix [36]
$\mathcal{P}_2$	60–650	1.45–3.25	68023.86048 ± 0.0432	974416624 ± 50	Abbott *et al.* [28]
$\mathcal{P}_3$	40–180	1.45–3.25	68023.86 ± 0.12	1178556229 ± 417	Zhang *et al.* [29]
$\mathcal{P}_4$	600–700				
$\mathcal{P}_5$	1000–1100				
$\mathcal{P}_6$	1400–1500	1.45–3.25	68023.70496 ± 0.0432	974416624 ± 100	Different ranges in frequency
$\mathcal{P}_7$	20–250				with broad range in a_p
$\mathcal{P}_8$	20–1000				
$\mathcal{P}_9$	20–1500				
$\mathcal{P}_{10}$	600–700				
$\mathcal{P}_{11}$	1000–1100				
$\mathcal{P}_{12}$	1400–1500	1.40–1.50	68023.70496 ± 0.0432	974416624 ± 100	Different ranges in frequency
$\mathcal{P}_{13}$	20–500				with narrow range in a_p
$\mathcal{P}_{14}$	20–1000				
$\mathcal{P}_{15}$	20–1500				
$\mathcal{P}_{16}$	600–700				
$\mathcal{P}_{17}$	1000–1100				
$\mathcal{P}_{18}$	1400–1500	1.44–1.45	68023.70496 ± 0.0432	974416624 ± 100	Different ranges in frequency
$\mathcal{P}_{19}$	20–500				with well-constrained a_p
$\mathcal{P}_{20}$	20–1000				
$\mathcal{P}_{21}$	20–1500				

AM, Prix, Wette (2023)

Different Observational Scenarios [contd …]

How Computing Cost Varies With Source Properties?

- Estimated a set of CW searches for different observational scenarios
- The source was a binary system
- Source parameters are 'Sco X-1' like, a well known LMXB system
- Estimated the computing cost for each of the search scenarios

TABLE II. Different search setups

Search setup	T_{obs} [months]	ΔT [days]	N	$\mu_{\max}$
`search setup-I`	6	1	180	0.031
`search setup-II`	12	3	120	0.056
`search setup-III`	6	3	60	0.025
`search setup-IV`	12	1	360	0.025
`search setup-V`	6	10	18	0.025
`search setup-VI`	12	10	36	0.025

AM, Prix, Wette (2023)

TABLE III. Computing-cost estimates $\mathcal{C}_{\mathcal{P}}$ (in million core hours [Mh]) for different parameter spaces $\mathcal{P}_n$ defined in Table I. We consider two setups, `search setup-I` and `search setup-II` of Table II, assuming either a 3D or 4D template bank.

	(I,3D)	(I,4D)	(II,3D)	(II,4D)
$\mathcal{P}_1$	3.18	23.51	3.93	43.23
$\mathcal{P}_2$	28.50	466.48	35.22	857.69
$\mathcal{P}_3$	5.00	63.40	6.17	116.57
$\mathcal{P}_4$	26.38	577.57	32.60	1061.95
$\mathcal{P}_5$	68.76	2425.79	84.96	4460.17
$\mathcal{P}_6$	131.09	6381.48	161.97	11733.30
$\mathcal{P}_7$	3.24	20.42	4.01	37.54
$\mathcal{P}_8$	207.74	5226.87	256.69	9610.37
$\mathcal{P}_9$	701.14	26461.02	866.33	48652.49
$\mathcal{P}_{10}$	0.90	11.65	1.12	21.42
$\mathcal{P}_{11}$	2.36	48.94	2.91	89.97
$\mathcal{P}_{12}$	4.49	128.73	5.55	236.70
$\mathcal{P}_{13}$	0.11	0.41	0.14	0.76
$\mathcal{P}_{14}$	7.12	105.44	8.80	193.87
$\mathcal{P}_{15}$	24.03	533.80	29.70	981.46
$\mathcal{P}_{16}$	0.09	1.16	0.11	2.13
$\mathcal{P}_{17}$	0.23	4.86	0.29	8.93
$\mathcal{P}_{18}$	0.45	12.78	0.55	23.50
$\mathcal{P}_{19}$	0.01	0.04	0.01	0.08
$\mathcal{P}_{20}$	0.71	10.47	0.88	19.25
$\mathcal{P}_{21}$	2.40	52.99	2.96	97.43